

# Effect of Relative Slip Amplitude on Fretting Fatigue Behavior of Silicon Nitride\*

Masaki OKANE\*\*, Toyochi SATOH\*\*\*,  
Yoshiharu MUTOH\*\*\*\* and Shogo SUZUKI\*\*\*\*\*

Fretting fatigue tests were carried out using HIP-sintered silicon nitride to study the effect of relative slip amplitude between the specimen and the contact pad on fretting fatigue behavior. Fretting fatigue strength decreased with increasing relative slip amplitude. Application of static contact without fretting motion had no influence on static fatigue strength. Therefore, fretting action with relative slip is essential for the degradation of fatigue strength. Fretting fatigue life prediction based on fracture mechanics analysis was also carried out, where the frictional force between the specimen and the contact pad was taken into consideration. The predicted fretting fatigue lives agreed well with the experimental results.

**Key Words:** Fatigue, Fretting Fatigue, Relative Slip Amplitude, Fracture Mechanics, Fatigue Life Prediction, Ceramics

## 1. Introduction

When ceramic materials are used in practical engineering applications, contact between ceramic components cannot be avoided in fits, joints and bearings. In these contacts, fretting damage, which results in a significant reduction of fatigue strength of these components, is often induced.

In our previous report<sup>(1)</sup>, a newly developed fretting fatigue test machine for ceramic materials was introduced, and preliminary results of fretting fatigue tests using HIP sintered silicon nitride were also

given. From the experimental results, it was found that fretting significantly reduced static fatigue strength of silicon nitride. Therefore, fretting fatigue behavior must be taken into consideration in the design or maintenance of ceramic components.

There are a large number of mechanical or metallurgical factors that affect fretting fatigue behavior. From a mechanical viewpoint, frictional force, relative slip amplitude and contact pressure are the major factors<sup>(2),(3)</sup>.

In this study, fretting fatigue tests were carried out using HIP sintered silicon nitride for both specimen and contact pad, to investigate the effect of relative slip amplitude on fretting fatigue behavior under static loading (static fretting fatigue). Fretting fatigue life prediction based on a fracture mechanics analysis, where the frictional force was taken into consideration, was also carried out.

## 2. Experimental Procedure

### 2.1 Materials

A HIP-sintered silicon nitride with as  $\text{Al}_2\text{O}_3$  and  $\text{Y}_2\text{O}_3$  additives was used for the test material, the Young's modulus, four-point bending strength,

\* Received 1st March, 1995. Japanese original: Trans. Jpn. Soc. Mech. Eng., Vol. 59, No. 566, A (1993), pp. 2220-2227. (Received 4th March, 1993)

\*\* Faculty of Engineering, Toyama University, 3190 Gofuku, Toyama 930, Japan

\*\*\* Technical Research and Development Institute, Japan Defence Agency, 1-2-10 Sakae, Tachikawa 190, Japan

\*\*\*\* Department of Mechanical Engineering, Nagaoka University of Technology, 1603-1 Kamitomioka, Nagaoka 940-21, Japan

\*\*\*\*\* Isuzu Ceramics Research Institute Co., Ltd., 8 Tsuchidana, Fujisawa 252, Japan

fracture toughness and hardness  $H_v$  of which are 304 GPa, 1000 MPa, 7.5 MPam<sup>1/2</sup> and 14 GPa, respectively. A rectangular bending test specimen was used as the fatigue specimen with dimensions of 3×4×36 mm and a cylindrical bar with diameter of 2 mm and length of 12 mm was used as the contact pad. A rectangular bar with dimensions of 5×10×55 mm was also machined from the same material as the static fatigue crack propagation specimen.

## 2.2 Fretting fatigue test

Fretting fatigue tests were carried out using a fretting fatigue test machine developed for ceramic materials. Details of the test machine were described in the previous report<sup>(1)</sup>. A schematic illustration of the test section (specimen setup) of the test machine is shown in Fig. 1. The oscillating motion of the cantilever beam and consequently of the specimen set in the test section was produced by an eccentric cam attached to the rotating driving shaft. The oscillating amplitude of the beam at the point where the test section was fixed was defined as  $S_{a,b}$  in this study, which is not always coincident with the relative slip amplitude  $S_a$  between the specimen and the contact pad due to the rigidity of the fixed jigs. In the present tests,  $S_{a,b}$  was controlled to obtain different levels of relative slip amplitude. Cylindrical contact pad was pressed onto a rectangular specimen by dead weight. Therefore, fretting occurs on the line contact surface between the specimen and the contact pad. In the fretting fatigue test, the specimen was maintained under a constant static fatigue stress by four-point bending (supporting span: 30 mm, loading span: 10 mm). The bending load was applied using the loading

bolt. The frictional force and the relative slip amplitude were measured during fretting fatigue tests using the strain gauges attached to the contact rod and the specially designed extensometer, respectively<sup>(1)</sup>.

Fretting fatigue tests were carried out under the conditions of  $S_{a,b}$  of 4 and 20 μm, frequencies of 5 and 10 Hz and contact load of 43 N. The test conditions are summarized in Table 1. As mentioned later, no significant effect of frequency on fretting fatigue strength was found in the present frequency range. Static fatigue tests without fretting contact (i.e., normal static fatigue tests) and static fatigue test with static contact but with no fretting action were also carried out to investigate the effect of fretting on fatigue strength.

Static fatigue strength and fretting fatigue strength were defined as the stress at which the specimen survives over the testing time of  $2 \times 10^5$  s, which corresponds to  $2 \times 10^6$  fretting cycles at 10 Hz.

## 2.3 Static fatigue crack propagation test

A static fatigue crack propagation test by three-point bending was carried out using a precracked rectangular specimen with dimensions of 5×10×55 mm to investigate the basic static fatigue properties of the material used. The precrack was induced by the BI (Bridge Indentation) method<sup>(4)</sup> and the crack propagation test was carried out following the method of Takahashi et al.<sup>(5)</sup> The stress intensity factor is given as<sup>(6)</sup>

$$K_{Ic} = \frac{3PS}{2Bh^2} \times \sqrt{\pi a} \cdot F\left(\frac{a}{h}\right) \quad (1)$$

$$F\left(\frac{a}{h}\right) = 1.090 - 1.753\left(\frac{a}{h}\right) + 8.20\left(\frac{a}{h}\right)^2 - 14.18\left(\frac{a}{h}\right)^3 + 14.57\left(\frac{a}{h}\right)^4$$

where  $a$  is the crack length,  $B$  the specimen thickness,  $h$  the specimen width,  $P$  the applied load and  $S$  the span length.

## 3. Results and Discussions

### 3.1 Fretting fatigue strength

The relationship between normalized applied stress and time to failure is shown in Fig. 2. Since several manufacturing lots of silicon nitride were used in this study, which have a 10% of scatter in bending strength, the applied stress was normalized by the average bending strength of each lot.

The  $S-T$  curves were very flat with a relatively large scatter. The strength of static fatigue without fretting contact (▼) at  $2 \times 10^5$  s was about 0.7 in  $\sigma_{max}/\sigma_{AB}$ . The strength of static fatigue with static contact (△) was almost equal to the static fatigue strength without fretting contact. The fracture occurred not always in the contact area but at any point in

Table 1 Test conditions

	Static fatigue without fretting	Static fatigue with static contact	Fretting fatigue (Static fatigue with fretting)	
Amplitude of cantilever beam $S_{a,b}$ , μm	-----	0	4	20
Frequency, Hz	-----	-----	5, 10	5, 10
Contact load $P$ , N	-----	43	43	43

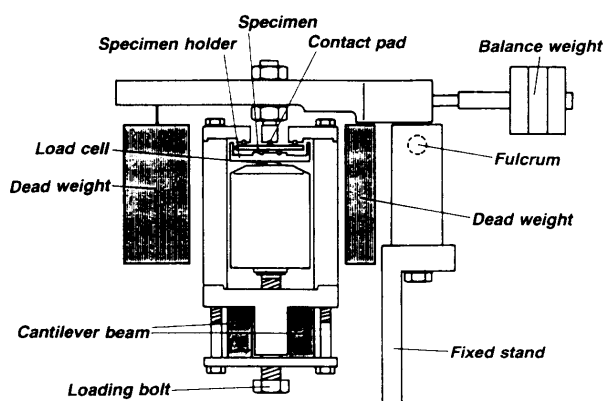


Fig. 1 Schematic illustration of the fretting fatigue test machine (magnified test section)

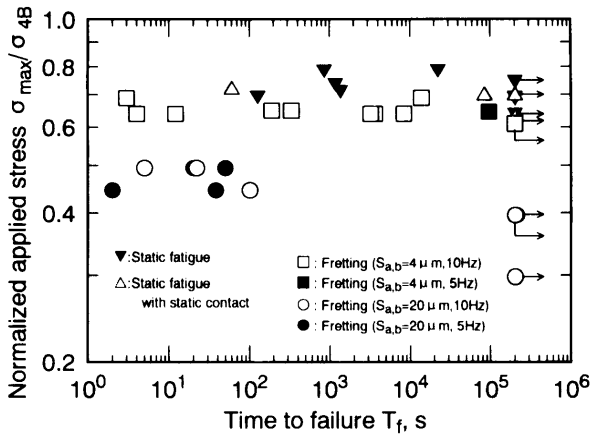


Fig. 2  $S$ - $T$  curves for fretting fatigue tests with cylindrical contact pad

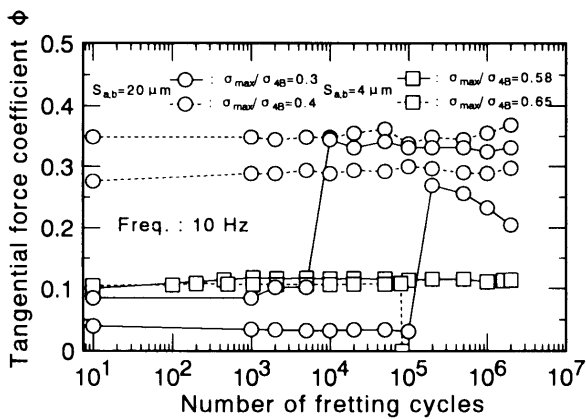


Fig. 3 Variation of tangential force coefficient for fretting fatigue tests with  $S_{a,b} = 4 \mu\text{m}$  and  $20 \mu\text{m}$

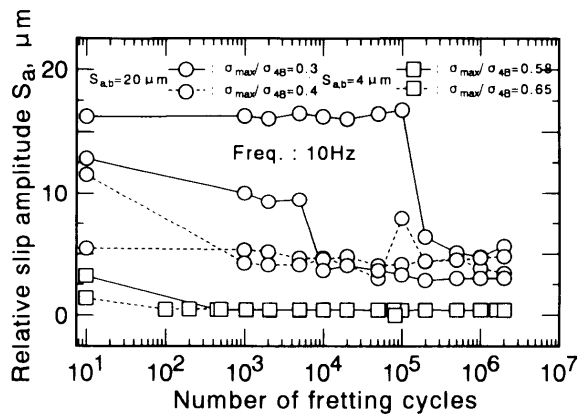


Fig. 4 Variation of relative slip amplitude for fretting fatigue tests with  $S_{a,b} = 4 \mu\text{m}$  and  $20 \mu\text{m}$

the loading span, which was similar to the behavior shown in the case of static fatigue test without fretting contact.

The fretting fatigue strength under a condition of  $S_{a,b} = 4 \mu\text{m}$  ( $\square$ ,  $\blacksquare$ ) was 0.62 in  $\sigma_{\max}/\sigma_{4B}$ . The fatigue lives under this condition were widely dispersed from about 30 s to  $10^4$  s.

The fretting fatigue strength under a condition of  $S_{a,b} = 20 \mu\text{m}$  ( $\circ$ ,  $\bullet$ ) was about 0.4 in  $\sigma_{\max}/\sigma_{4B}$ . In this condition the fatigue lives were rather short and concentrated in  $10^2$  s, which indicated that the initiation and propagation of fretting cracks (fretting damage) occurred at a very early stage of the test. Fracture points of the specimen in all fretting fatigue tests were in the contact area.

Fretting significantly reduced the fatigue strength of silicon nitride, and fretting fatigue strength decreased with increasing slip amplitude  $S_{a,b}$ . In the case of the static fatigue test with static contact, no frictional force is produced on the contact surfaces. The fatigue strengths of the two static fatigue tests coincide regardless of static contact. This result suggests that frictional force by fretting action significantly influences the static fatigue behavior of silicon nitride.

### 3.2 Tangential force coefficient and relative slip amplitude

Variations of tangential force coefficient and relative slip amplitude against the number of fretting cycles are shown in Figs. 3 and 4, respectively. The tangential force coefficient was defined as the ratio of frictional force  $F$  to contact load  $P$ ,  $F/P$ . The tangential force coefficient  $F/P$  increases with increasing relative slip amplitude  $S_a$ , and attains a constant value which corresponds to the coefficient of friction  $\mu$ , when gross slip occurs.

Tangential force coefficient, i.e., frictional force and relative slip amplitude under the condition of  $S_{a,b} = 4 \mu\text{m}$  showed constant values during the fretting fatigue test, which were smaller than those under the condition of  $S_{a,b} = 20 \mu\text{m}$ . A sudden increase in tangential force coefficient and a simultaneous sudden decrease in relative slip amplitude were observed in the specimen tested under conditions of  $\sigma_{\max}/\sigma_{4B} = 0.3$  and  $S_{a,b} = 20 \mu\text{m}$ . The attained higher value of tangential force coefficient and lower value of relative slip amplitude coincided with those of the specimen tested under the higher applied stress  $\sigma_{\max}/\sigma_{4B} = 0.4$ .

This transition behavior of the tangential force coefficient and the relative slip amplitude may have resulted from the change of fretted surface morphology. The higher applied stress easily induces the initiation and propagation of delaminating cracks and drop-out of the particles. Therefore, it seems that severe surface damage occurred in the contact region at a very early stage of the test under the stress level of  $\sigma_{\max}/\sigma_{4B} = 0.4$ , while under the stress level of  $\sigma_{\max}/\sigma_{4B} = 0.3$  surface damage was not severe until the transition behavior occurred.

From the results of fretting wear tests of silicon nitride contact to same kind of silicon nitride<sup>(7)</sup>, it was

seen that the coefficient of friction (tangential force coefficient) gradually increases around up to 0.8 with increasing relative slip amplitude from  $14\ \mu\text{m}$  to  $290\ \mu\text{m}$ . The value of 0.8 is almost equal to the coefficient of friction of silicon nitride measured by a pin-on-disk-type wear test<sup>(8)</sup>. The coefficient of friction of the present silicon nitride was about 0.7, as will be discussed later. Tangential force coefficients during the fretting fatigue tests were smaller than 0.7. Therefore, not gross slip but partial slip is expected to occur in the contact region.

### 3.3 SEM observations of fretted surface

SEM micrographs of the fretted surfaces are shown in Fig. 5. It is clear that fretting damage is more severe and the width of the fretted region is larger under the condition of  $S_{a,b} = 20\ \mu\text{m}$  than under the condition of  $S_{a,b} = 4\ \mu\text{m}$ . Considerable amount of wear debris was observed for  $S_{a,b} = 20\ \mu\text{m}$ , while no debris was found for  $S_{a,b} = 4\ \mu\text{m}$ . Faded contact marks were observed in the specimen tested under static fatigue with static contact, as shown in Fig. 6, where the observation was conducted from a 45-degree oblique direction in order to clearly observe the marks. The fracture points under static fatigue with static contact were dispersed in the loading span and not always concentrated in the contact area. Therefore, the present level of contact load caused no serious surface damage and did not influence static fatigue strength. Consequently, the fretting action, which induces frictional force on the contact surface and contributes to the initiation and propagation of fretting cracks, is found to play an essential role in fretting fatigue.

### 3.4 Relationship between fretting fatigue strength and relative slip amplitude

In metallic materials, fretting fatigue strength

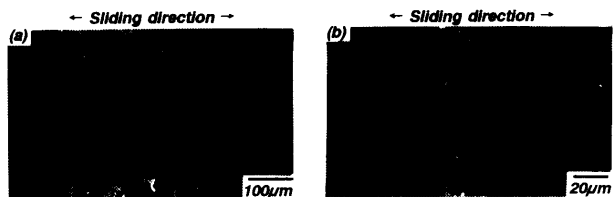


Fig. 5 SEM micrographs of the fretted surface tested up to  $2 \times 10^6$  cycles. (a)  $\sigma_{\max}/\sigma_{4b} = 0.3$ ,  $S_{a,b} = 20\ \mu\text{m}$ ; (b)  $\sigma_{\max}/\sigma_{4b} = 0.58$ ,  $S_{a,b} = 4\ \mu\text{m}$



Fig. 6 An SEM micrograph of the contact surface under the condition of static fatigue with static contact

decreases with increasing relative slip amplitude because the frictional force between the specimen and the contact pad increases with increasing relative slip amplitude<sup>(9)</sup>. Furthermore, the frictional force becomes constant above the critical value of relative slip amplitude where gross slip occurs, and hence the fretting fatigue strength also becomes constant<sup>(9)</sup>. In the present material, the same behavior was observed, as shown in Fig. 7. The normalized fretting fatigue strength  $\sigma_{wf}/\sigma_{4b}$  initially decreased with increasing relative slip amplitude and then became constant.

## 4. Fretting Fatigue Life Prediction Based on Fracture Mechanics Analysis

Based on previous interrupted fretting fatigue test results<sup>(1)</sup> and the present results, the fretting fatigue fracture process in silicon nitride is assumed to be as follows. Fretting cracks initiate at a very early stage of fatigue life and propagate at an accelerated growth rate due to frictional force. In the following analysis, fretting lives were estimated based on a fracture mechanics model of a fretting fatigue crack.

### 4.1 Stress intensity factor of a fretting fatigue crack

The stress intensity factor of a crack at the edge in half-plane, which is affected by the tangential force along the edge surface, as shown in Fig. 8, was derived

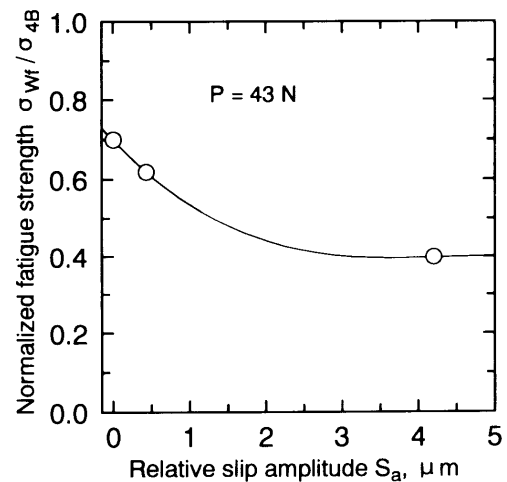


Fig. 7 Relationship between relative slip amplitude and normalized fatigue strength

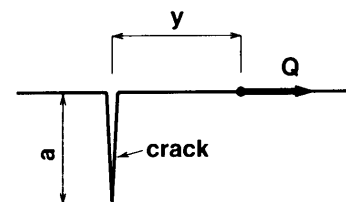


Fig. 8 A crack at the edge in half plane which is affected by the tangential force along the edge surface

by Rooke and Jones<sup>(10)</sup>. The mode I stress intensity factor  $K_{Iq}$  is given by the following equation.

$$K_{Iq} = \frac{Q}{\sqrt{\pi a}} (1 - \xi^2) [1.2943 + 0.0044\xi + 0.1289\xi^2 + 10.89\xi^3 - 22.14\xi^2 + 10.96\xi^5] \quad (2)$$

where  $\xi = y/(y + a)$ ,  $a$  is the crack length,  $Q$  is the tangential force per unit length along the edge surface and  $y$  is the distance from the crack to the point of applied tangential force. When the tangential force  $Q$  is given in the form of a distribution  $q(y)$ , the stress intensity factor is calculated by integrating Eq.(2) over the contact area.

Silicon nitride behaves as an elastic body under a condition of tensile stress. However under a condition of compressive stress, such as in an indentation test it is well known that plastic deformation occurs. Since the present level of contact load seems to be insufficient for plastic deformation, the contact stress state may be assumed as the Hertzian elastic contact<sup>(11)</sup>. The contact half-width  $b$  in the case that a cylinder is pressed onto a plane of the same material is given as

$$b = \sqrt{\frac{8}{\pi} W r \cdot \left[ \frac{1 - \nu^2}{E} \right]} \quad (3)$$

where  $W$  is the contact load per thickness,  $r$  is the radius of cylinder, and  $E$  and  $\nu$  are Young's modulus and Poisson's ratio, respectively. The contact pressure distribution  $P(\eta)$  is given by the following equation, where  $\eta$  is the coordinate on the contact surface, the origin of which is the center of the contact area.

$$P(\eta) = \frac{2W}{\pi b} \cdot \sqrt{1 - \left(\frac{\eta}{b}\right)^2} \quad (4)$$

For the case that tangential force is applied to a Hertzian contact, the frictional stress distribution on the contact surface was derived by Mindlin and Deresiewicz<sup>(12)</sup>. They defined two regions in the contact area, i.e., the stick region and the slip region. The distribution of frictional stress along the contact surface is given by

$$q(\eta) = -\mu P_{\max} \cdot \sqrt{1 - \left(\frac{\eta}{b}\right)^2} + q'(\eta) \quad (5)$$

where

$$b \geq |\eta| \geq c : q'(\eta) = 0$$

$$|\eta| < c : q'(\eta) = \mu P_{\max} \frac{c}{b} \sqrt{1 - \left(\frac{\eta}{c}\right)^2}$$

$\mu$  is the coefficient of friction,  $P_{\max}$  is the maximum Hertzian pressure calculated by Eq.(4), and  $c$  is the distance to the boundary between the stick region and the slip region, which is given by the following equation.

$$\frac{c}{b} = \sqrt{1 - \left(\frac{Q}{\mu W}\right)} \quad (6)$$

The coefficient of friction  $\mu$  of the present material was measured using the fretting fatigue test

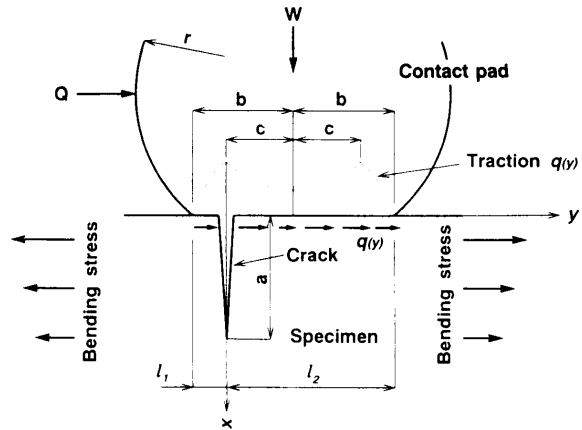


Fig. 9 The fracture mechanics model of a fretting fatigue crack

machine under the gross slip condition without stress applied to the specimen. The obtained value was 0.68.

The fracture mechanics model of a fretting fatigue crack assumed in the present study is shown in Fig. 9. Assumptions for this model are follows.

(1) The distribution of traction (frictional stress) is given by the Mindlin's solution as shown by the broken line in Fig. 9.

(2) The initial crack is through-thickness and perpendicular to the specimen surface, and its size is of the same order as the grain size (5  $\mu\text{m}$ ).

(3) The fretting fatigue crack initiates at the boundary between the stick region and the slip region, where the traction stress is maximal.

(4) Although the contact load may have some influence by way of mean stress on crack propagation behavior, the mean stress effect due to contact load can be assumed to be negligible under the present fretting fatigue condition.

(5) The fretting fatigue crack propagates in static fatigue crack growth manner, while the frictional force is cyclic.

The stress intensity factor due to frictional force  $K_{\text{fric}}$  is given by integrating Eq.(2) over the contact surface, where the  $\eta$  coordinate in Eq.(5) transforms to the  $y$ -coordinate.

$$K_{\text{fric}} = - \int_{y=-l_1}^{y=0} K_{Iq(y)} dy + \int_{y=0}^{y=l_2} K_{Iq(y)} dy \quad (7)$$

where the origin of  $x$ - $y$  coordinates is set at the crack end on the surface, as shown in Fig. 9, and  $l_1$  and  $l_2$  are the distances from the origin of the coordinates to each edge of the contact area.

The stress intensity factor due to applied four-point bending  $K_{\text{app}}$  is given as<sup>(6)</sup>

$$K_{\text{app}} = \sigma_{\max} \sqrt{\pi a} \cdot F_1 \left( \frac{a}{h} \right) \quad (8)$$

$$F_1 \left( \frac{a}{h} \right) = 1.122 - 1.40 \left( \frac{a}{h} \right) + 7.33 \left( \frac{a}{h} \right)^2$$

$$-13.08\left(\frac{a}{h}\right)^3 + 14.0\left(\frac{a}{h}\right)^4$$

where  $\sigma_{\max}$  is the maximum bending stress and  $h$  is the specimen width.

Therefore, the stress intensity factor for a fretting fatigue crack  $K_{\max}$  is given by combining Eqs. (7) and (8).

$$K_{\max} = K_{\text{app}} + K_{\text{fric}} \quad (9)$$

From our previous test results<sup>(1)</sup>, the contact was not necessarily uniform in the specimen thickness direction, and some microscopic non-contact regions were observed along the contact line. This may have resulted from the unavoidable waviness of the finished surfaces of specimens and contact pads. Therefore, the frictional force did not uniformly distribute along the contact line but concentrated in several localized contact areas. The contact ratio CR is defined as the ratio of real contact length to the specimen thickness (the apparent contact length). CR was used for estimating the frictional force on the real contact area and calculating the  $K_{\text{fric}}$  due to the frictional force.

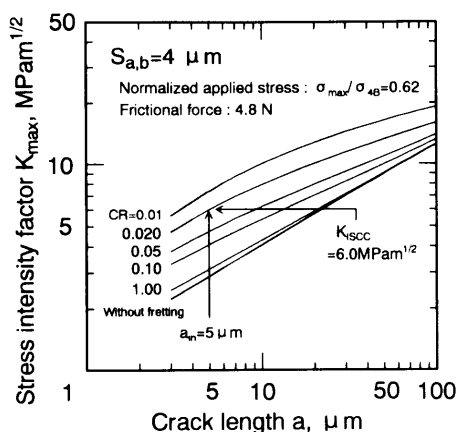
Relationships between crack length and the esti-

mated stress intensity factor are shown in Fig. 10. The mean frictional force values of 14.0 N for the condition of  $S_{a,b}=20 \mu\text{m}$  and 4.8 N for  $S_{a,b}=4 \mu\text{m}$  were used in the calculation. It is clear from the figure that the stress intensity factors for fretting fatigue cracks are higher than those for normal fatigue cracks, especially when a crack length is short. In other words, the crack propagation rate is significantly accelerated in the early stage of crack propagation. It is also found that the  $K$  value increases with decreasing CR. From a comparison of Figs. 10(a) and (b), the  $K$  values increase with increasing  $S_{a,b}$  (i.e., relative slip amplitude  $S_a$ ). This results from the frictional force increasing with increasing  $S_{a,b}$ .

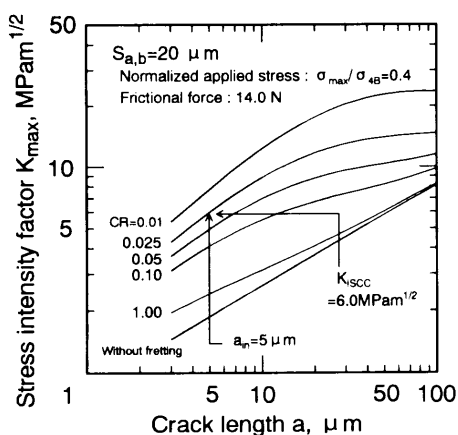
The fretting fatigue limit corresponds to the critical stress level necessary to arrest a fretting fatigue crack<sup>(13)</sup>.  $\text{CR}_{\text{th}}$  is defined as the maximum value of CR at which the stress intensity factor of a fretting fatigue crack with length of  $5 \mu\text{m}$  coincides with the threshold stress intensity factor for static fatigue crack propagation  $K_{\text{ISCC}}$ . Relationships between  $\text{CR}_{\text{th}}$  and the normalized applied stress  $\sigma_{\max}/\sigma_{4B}$  are shown in Fig. 11. It is clear that  $\text{CR}_{\text{th}}$  increases with increasing  $\sigma_{\max}/\sigma_{4B}$ . The normalized fretting fatigue strength of the present material  $\sigma_{wf}/\sigma_{4B}$  was 0.40 for  $S_{a,b}=20 \mu\text{m}$  and 0.62 for  $S_{a,b}=4 \mu\text{m}$ . The values of  $\text{CR}_{\text{th}}$  at these stress levels were 0.025 for  $S_{a,b}=20 \mu\text{m}$  and 0.020 for  $S_{a,b}=4 \mu\text{m}$ , and were used in the following fretting fatigue life prediction.

#### 4.2 Fretting fatigue life prediction

The relationship between crack propagation rate  $da/dt$  and stress intensity factor  $K_{\max}$  can be expressed in the following equation, which is modified using the threshold stress intensity factor for static fatigue crack propagation  $K_{\text{ISCC}}$ .



(a)



(b)

Fig. 10 Relationship between crack length and the stress intensity factor. (a)  $S_{a,b} = 4 \mu\text{m}$ , (b)  $S_{a,b} = 20 \mu\text{m}$

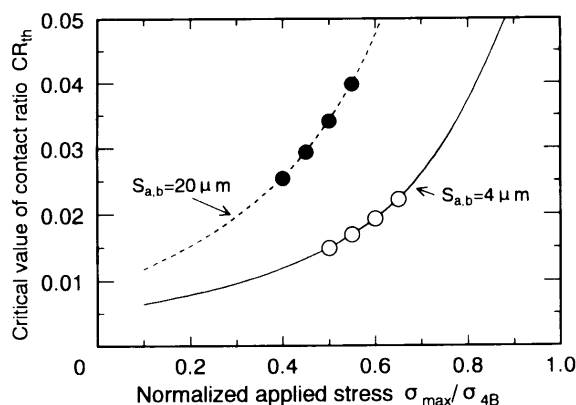


Fig. 11 Relationship between normalized applied stress and critical value of contact ratio

$$\frac{da}{dt} = C_0(K_{\max}^m - K_{\text{ISCC}}^m), \quad (10)$$

where  $C_0$  and  $m$  are material constants. The values of  $K_{\text{ISCC}}$ ,  $C_0$  and  $m$  of the present material were  $6.0 \text{ MPa}\sqrt{m}$ ,  $3.11 \times 10^{-37}$  and 35.7, respectively. Fretting fatigue life can be calculated by integrating Eq.(10). The initial crack length  $a_{\text{in}}$  was assumed to be  $5 \mu\text{m}$ , as mentioned in assumption (2). Further investigations are necessary to clarify whether the assumed initial crack length is proper or not. The terminating crack length  $a_f$  was estimated based on the fracture toughness  $K_{\text{IC}}$  of the present material ( $7.5 \text{ MPa}\sqrt{m}$ ).

The result of fretting fatigue life prediction is shown in Fig. 12. The predicted fretting fatigue lives agreed well with the experimental results. The experimental results showed wide scatter around the predicted life. This may result from the scatters of static fatigue lives without fretting and initial values of CR, and also from the variation of CR during the test.

It seemed that CR in the early stage of the test was very small, as shown in Fig. 6 and subsequently the CR increased with developing fretting wear. Therefore, fretting wear region of the specimens tested up to  $2 \times 10^5 \text{ s}$  was extended uniformly along the contact line, as shown in Fig. 5. Although the CR values used in the prediction correspond to those in the early stage of the test, where the crack growth is significantly accelerated, they do not coincide with those observed on the specimen tested for a long period.

From our previous results<sup>(1)</sup>, the length of a surface crack observed in the early stage of the test was approximately  $70 \mu\text{m}$ . The ratio of the crack length to the apparent contact length (4 mm) was 0.018, which indicated that the assumed CR values were reasonable.

To discuss the assumption of CR further, a fretting fatigue test was carried out using the HIP-sintered silicon nitride spherical contact pad with a diameter of  $D=5/32 \text{ in.}$  ( $3.97 \text{ mm}$ ), under a contact load of  $P=43 \text{ N}$ , a normalized applied stress  $\sigma_{\max}/\sigma_{4B}=0.65$  and a frequency of 10 Hz. The  $S_{a,b}$  value for the test with spherical contact pad was controlled to be  $2 \mu\text{m}$  to coincide the frictional force with that for the test with cylindrical contact pad where  $S_{a,b}=4 \mu\text{m}$ . The relative slip amplitude  $S_a$  measured in the test with a spherical contact pad was  $0.68 \mu\text{m}$ , which almost coincided with that measured during the tests with the cylindrical contact pad.

The test result is plotted in Fig. 12 by  $\blacklozenge$ . The fretting fatigue life was rather long but within the scatter of fretting fatigue lives for the test with the cylindrical contact pad. The average value of fric-

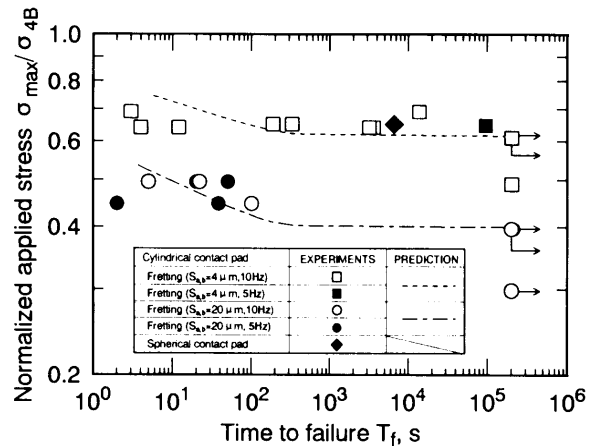


Fig. 12 Predicted S-curves

tional force was 4.1 N, which was relatively low compared to that for the cylindrical contact pad (4.8 N). The diameter of the elastic contact area was about  $150 \mu\text{m}$  based on Hertzian theory<sup>(11)</sup>. The ratio of the diameter of elastic contact to the specimen thickness was 0.038, which was larger than the critical value of contact ratio  $\text{CR}_{\text{th}}$  for the cylindrical contact pad (0.020). Although there are some geometrical differences in contact between cylindrical and spherical contact pads, which result in the lower frictional force and higher contact ratio for the spherical contact pad, the fretting fatigue lives almost coincide with each other. Therefore, it seems to be reasonable that uniform initial contact is not achieved along the contact line between the specimen and the cylindrical contact pad, and that the frictional force is concentrated on some localized contact regions.

## 5. Conclusions

Fretting fatigue tests of HIP-sintered silicon nitride with various slip amplitudes were carried out. The main results obtained are summarized as follows.

(1) The static fatigue strength of silicon nitride was reduced by fretting action. The fretting fatigue strength decreased with increasing relative slip amplitude.

(2) The frictional force between the specimen and the contact pad increased with increasing relative slip amplitude.

(3) Application of static contact without fretting motion had no influence on static fatigue strength. Therefore, the surface damage (wear) and the frictional force due to fretting action result in the degradation of static fatigue strength.

(4) The predicted fretting fatigue lives based on the fracture mechanics analysis, where the frictional force was taken into consideration, agreed well with the experimental results. The experimental fatigue

lives were widely dispersed around the predicted lives. This experimental dispersion results from the fact that the static fatigue lives tend to scatter widely and that the concentration ratio of the frictional force in the localized real contact regions, that is, the contact ratio CR, scatters depending on the combination of specimen and contact pad used.

#### Acknowledgement

This study was supported by a Grant-in-Aid for Scientific Research (No. 04650062) from the Ministry of Education, Science and Culture, Japan.

#### References

- (1) Okane, M., Satoh, T., Mutoh, Y. and Suzuki, S., Trial Construction of a Fretting Fatigue Test Machine for Ceramic Materials and Preliminary Test Results, *Trans. Jpn. Soc. Mech. Eng.*, (in Japanese), Vol. 59, No. 561, A (1993), p. 1384.
- (2) Nishioka, K. and Hirakawa, K., Fundamental Investigation of Fretting Fatigue. Part 5-The Effect of Relative Slip Amplitude, *Trans. Jpn. Soc. Mech. Eng.*, (in Japanese), Vol. 34, No. 268, (1968), p. 2068.
- (3) Nagata, K., Matsuda, K. and Kashiwaya, H., Effect of Contact Pressure on Fretting Fatigue Strength, *Trans. Jpn. Soc. Mech. Eng.*, (in Japanese), Vol. 53, No. 486, A (1987), p. 196.
- (4) Sadahiro, T. and Takatsu, S., A New Precracking Method for Fracture Toughness Testing of Cemented Carbides, *Modern Develop. Powder Metall.*, (1981), 12~14, p. 561.
- (5) Takahashi, M., Mutoh, Y., Okamoto, H. and Oikawa, T., Long and Short Fatigue Crack Growth Behavior in Silicon Nitride, *J. Soc. Mater. Sci. Japan*, (in Japanese), Vol. 40 (1991), p. 588.
- (6) Brown, W. F. Jr. and Srawley, J. E., Plane Strain Crack Toughness Testing of High Strength Metallic Materials, *ASTM STP 410*, (1966), p. 12.
- (7) Satoh, J., Shima, M. and Takeuchi, M., Fretting Wear in Seawater, *Wear*, 110, (1986), p. 227.
- (8) Sasaki, S., The Effect of Water on Friction and Wear of Ceramics, *Journal of Japanese Society of Lubrication Engineers*, (in Japanese), Vol. 33, No. 8 (1988), p. 620.
- (9) Mutoh, Y., Nishida, T. and Sakamoto, I., Effect of Relative Slip Amplitude and Contact Pressure on Fretting Fatigue Strength, *J. Soc. Mater. Sci. Japan*, (in Japanese), Vol. 37 (1988), p. 649.
- (10) Rooke, D. P. and Jones, D. A., Stress Intensity Factor in Fretting Fatigue, *J. Strain Analysis*, Vol. 14, No. 1 (1979), p. 1.
- (11) Hertz, H., Über die berührung fester elastischer Körper, *J. für die reiner. angew. mathem.*, 92 (1881), p. 156
- (12) Mindlin, R. D. and Deresiewicz, H. D., Elastic Sphere in Contact under Oblique Force, *J. App. Mech.*, September, (1949), p. 327.
- (13) Tanaka, K., Mutoh, Y. and Sakoda, S., Effect of Contact Materials on Fretting Fatigue in a Spring Steel, *Trans. Jpn. Soc. Mech. Eng.*, (in Japanese), Vol. 51, No. 464, A (1985), p. 1200.